Evidence for Unfolding of the Single-Stranded GCCA 3'-End of a tRNA on Its Aminoacyl-tRNA Synthetase from a Stacked Helical to a Foldback Conformation †

4 AUTHORS, INCLUDING:

Jacques Lapointe
Laval University

110 PUBLICATIONS **2,214** CITATIONS

Evidence for Unfolding of the Single-Stranded GCCA 3′-End of a tRNA on Its Aminoacyl-tRNA Synthetase from a Stacked Helical to a Foldback Conformation[†]

Eric Madore,[‡] Richard S. A. Lipman,[§] Ya-Ming Hou,[§] and Jacques Lapointe*,[‡]

Département de Biochimie et de Microbiologie, Centre de Recherche sur la Fonction, la Structure et l'Ingénierie des Protéines (CREFSIP), Faculté des Sciences et de Génie, Université Laval, Québec, Canada, G1K 7P4, and Department of Biochemistry and Molecular Pharmacology, Thomas Jefferson University, Philadelphia, Pennsylvania 19107

Received October 25, 1999; Revised Manuscript Received April 5, 2000

ABSTRACT:　The conformation of a tRNA in its initial contact with its cognate aminoacyl-tRNA synthetase was investigated with the *Escherichia coli* glutamyl-tRNA synthetase−tRNA^{Glu} complex. Covalent complexes between the periodate-oxidized tRNA^{Glu} and its synthetase were obtained. These complexes are specific since none were formed with any other oxidized *E. coli* tRNA. The three major residues cross-linked to the 3′-terminal adenosine of oxidized tRNA^{Glu} are Lys115, Arg209, and Arg48. Modeling of the tRNA^{Glu}−glutamyl-tRNA synthetase based on the known crystal structures of *Thermus thermophilus* GluRS and of the *E. coli* tRNA^{Gln}−glutaminyl-tRNA synthetase complex shows that these three residues are located in the pocket that binds the acceptor stem, and that Lys115, located in a 26 residue loop closed by coordination to a zinc atom in the tRNA acceptor stem-binding domain, is the first contact point of the 3′-terminal adenosine of tRNA^{Glu}. In our model, we assume that the 3′-terminal GCCA single-stranded segment of tRNA^{Glu} is helical and extends the stacking of the acceptor stem. This assumption is supported by the fact that the 3′ CCA sequence of tRNA^{Glu} is not readily circularized in the presence of T4 RNA ligase under conditions where several other tRNAs are circularized. The two other cross-linked sites are interpreted as the contact sites of the 3′-terminal ribose on the enzyme during the unfolding and movement of the 3′-terminal GCCA segment to position the acceptor ribose in the catalytic site for aminoacylation.

Before its incorporation into proteins in vivo, each amino acid is first activated by a specific aminoacyl-tRNA synthetase (aaRS)[1] in the presence of ATP, yielding an aminoacyl-adenylate−aaRS noncovalent complex which can then transfer the activated aminoacyl group to a tRNA substrate. It was shown that the ligand-free tRNA for some species is not the same as the synthetase-bound tRNA. Comparison of the free and synthetase-complexed tRNA^{Asp} revealed important changes in the anticodon stem and loop, and small changes in the acceptor stem (*1, 2*). Important conformationnal differences were also observed between complexed tRNA^{Gln}, free tRNA^{Asp}, and free tRNA^{Phe}. These differences are in the acceptor stem and in the anticodon stem and loop (*1−4*). Little is known about the conformation of tRNAs during their initial contact with their cognate aaRS,

and about the subsequent changes that lead to the form for aminoacylation. To investigate the conformation of the single-stranded CCA-end of tRNA during aminoacylation, we chose the *E. coli* tRNA^{Glu}−glutamyl-tRNA synthetase (GluRS) complex.

We report here that covalent complexes were formed during the interaction of this enzyme with the periodate-oxidized tRNA^{Glu}. The three major residues cross-linked to the 3′-terminal modified ribose were located in a cleft that is predicted to bind the tRNA acceptor stem. This prediction is based on molecular modeling of *E. coli* GluRS according to the known 3D structure of *Thermus thermophilus* GluRS (*5*) and that of the *E. coli* tRNA$_2^{Gln}$−glutaminyl-tRNA synthetase (GlnRS) complex (*4*). Due to the predicted stiffness of the GCCA end of *E. coli* tRNA^{Glu}, we propose that one of these sites corresponds to the initial contact of GluRS with the terminal ribose of tRNA^{Glu} with its single-stranded 3′-end in the helical conformation and stacked on the acceptor stem. We propose that the remaining two cross-linked residues show the pathway of the CCA end during its movement toward the active site of the enzyme.

EXPERIMENTAL PROCEDURES

Materials. E. coli GluRS was purified from the overproducing strain DH5α(pLQ7612), as previously described (*6*). The fully modified *E. coli* tRNA^{Glu} was purified from *E. coli* DH5α containing the overproducing plasmid pKR15 (kindly provided by Dr. Kelley Rogers and Dr. Dieter Söll)

by phenol extraction followed by chromatography on monoQ and on a modified ODS-Hypersyl column (*7*). Unfractionated *E. coli* tRNA enriched for $tRNA_2^{Gln}$ was purified from *E. coli* K12ΔH1ΔTrp/pRS3 as described by Perona et al. (*8*).

Cross-Linking. *E. coli* tRNA^{Glu} was labeled on its 3′-terminal phosphate using [α-^{32}P]ATP and the tRNA nucleotidyl transferase purified from the overproducing *E. coli* strain UT481/pEC7 kindly provided by Dr. Murray P. Deutscher (*9*). Periodate oxidation of tRNA^{Glu} was performed as described by Fayat et al. (*10*). Nonequilibrium reaction of periodate-oxidized *E. coli* tRNA^{Glu} (tRNA$_{OX}^{Glu}$) (2 mg) and of *E. coli* GluRS (2 mg) was conducted for 1 h at 37 °C in 500 μL of 20 mM imidazole, pH 8.0, 10 mM MgCl₂, 25% glycerol, and 10 mM NaCNBH₃. Periodate oxidation modifies no other part of tRNA^{Glu} besides the 3′-terminal ribose (*11*). Equilibrium assay was performed under the same conditions without NaCNBH₃. The reaction was stopped by the addition of 0.2 volume of 0.5 M NaBH₄ in 10 mM NaOH. NaBH₄, like NaCNBH₃, stabilizes Schiff bases and, unlike NaCNBH₃, reduces oxidized tRNA (*12*, *13*).

Purification and Characterization of the Covalent tRNA$_{OX}^{Glu}$−GluRS Complexes. The complexes were separated by electrophoresis in the presence of SDS in 10% polyacrylamide gels (*14*). The gel sections containing complexes were cut, ground, placed in dialysis bags (Spectra/Por, Fisher #08-667E) containing 25 mM Tris, 250 mM glycine, pH 8.3, and 0.1% SDS, and submitted to electrophoresis in the same buffer. After 2 h of electrophoresis at 4 °C, the contents of the bags were passed through fritted glass filters to remove acrylamide. The volume of this solution was reduced to 50 μL by filtration with a Centricon-30 (from Amicon), and the concentration of SDS was reduced to 0.01% by successive dilutions and filtrations. The molecular mass of the tRNA$_{OX}^{Glu}$−GluRS complexes was determined by electrophoresis on polyacrylamide gels of various concentrations under nondenaturing conditions (*15*), and by ESI (electrospray ionization) mass spectrometry. The latter was performed on a Micromass Quattro II triple-stage quadrupole mass spectrometer (Micromass, U.K.) by Dr. Gilles Lajoie and Dr. Jian Chen at the Biological Mass Spectrometry Laboratory, University of Waterloo, Waterloo, Ontario, Canada.

Isolation of the Tryptic Peptides Cross-Linked to the Oxidized 3′-Terminal A of tRNA^{Glu}. The tRNA present in the complexes was digested using 100 units of RNase T1 (from Boehringer Mannheim) for 3 h at 37 °C in the 0.01% SDS buffer described above. The buffer was changed to 100 mM ammonium bicarbonate, pH 8.0, using a Centricon-30. The GluRS was then digested with trypsin (T-013H from Sigma) at a ratio of 1:20 (w/w) for 24 h at 37 °C. About 15 μmol of peptides was put on a 20 cm × 20 cm cellulose plate (no. 6064 from Kodak). The first migration was achieved by ascending chromatography in ethanol/chloroform/28% ammonia/water (5:2:1:1), and the second one by electrophoresis in 100 mM ammonium acetate, pH 8, in a Savant TLE20 apparatus. The peptides were colored with 0.2% ninhydrin and 2% trimethylpyridine, or revealed by autoradiography. The radioactive spots on the plate were cut off, and the peptides were extracted first with water and then with 50% (v/v) acetonitrile in water. Extracted peptides were concentrated and sequenced by Edman degradation.

Examination of the Stacked Helical Conformation of the GCCA End by tRNA Circularization. The standard conditions for circularization have been described (*16*). The native tRNA^{Glu} isolated from *E. coli* and the T7 transcript of *E. coli* tRNA^{Cys} and of its A73 variant were labeled at the 5′-end with [γ-^{32}P]ATP according to a published procedure (*17*). The labeled tRNA was separated from the free label by a 12% polyacrylamide/7 M urea gel and was extracted from the gel and ethanol-precipitated. The specific activity of the labeled tRNA was approximately 10⁴ cpm/80 pmol. Prior to the circularization reaction, 80 pmol of a labeled tRNA was denatured at 80 °C for 3 min and annealed at room temperature for 5 min in 50 mM NaCl, 10 mM sodium phosphate, pH 6.5, and 0.1 mM EDTA. The annealed tRNA was then adjusted to 16 μM in 24 μL with the addition of 50 mM ATP, 12.5% DMSO, 50 mM Tris-HCl, pH 7.5, 10 mM MgCl₂, 2 mM DTT, and 0.375 unit/μL T4 RNA ligase (Pharmacia). After incubation at 16 °C for various lengths of time, an aliquot was removed, loaded on a 12% denaturing polyacrylamide/7 M urea gel, and electrophoresed at 1800 V for 5 h in TBE buffer (89 mM Tris−borate, 89 mM borate, 2 mM EDTA). The circular tRNA migrated slower than the linear tRNA, and the amount of circularization was quantitated by phosphorimage analysis.

Molecular Modeling. Modeling was performed on a Indigo 2 Silicon Graphic workstation using the InsightII software from Biosym Technologies. Visualization was made using Roger Sayle's RasMol software from Glaxo Wellcome Research and Development. Sequence analyses were performed using the Wisconsin Package (Version 9.0) Genetics Computer Group (GCG), Madison, WI (*18*).

RESULTS AND DISCUSSION

Covalent Complexes between E. coli GluRS and Periodate-Oxidized tRNA^{Glu}. SDS−PAGE analysis of the products of the reaction between oxidized tRNA^{Glu} and GluRS revealed the formation of two complexes (Figure 1-I, lane A1). Their molecular masses are respectively about 73 kDa (complex 1) and 94 kDa (complex 2), as determined by electrophoresis under nondenaturing conditions in polyacrylamide gels of various porosities (Figure 1-III) and confirmed by ESI mass spectrometry (Figure 1-II). Therefore, these complexes contain one GluRS (53.8 kDa) and respectively one and two tRNA^{Glu} (25.5 kDa). On the mass spectrum, the major peak corresponds to the 1:2 complex (104.5 kDa) and the second highest to the 1:1 complex (79.95 kDa); other peaks come from RNA fragmentation (reviewed in *19*). The same complexes were obtained when we used unfractionated tRNA instead of pure tRNA^{Glu} (Figure 1-I, lane A2). To make sure that the complex was not formed between GluRS and tRNA^{Gln} or any other tRNAs, we performed the following controls. We prepared total tRNA from a strain that overproduced tRNA^{Gln} (*E. coli* K12ΔH1ΔTrp/pRS3) and subjected this tRNA to aminoacylation with glutamate. The rationale was that aminoacylation would protect tRNA^{Glu} from oxidation such that it would prevent tRNA^{Glu} from complex formation with GluRS (Figure 1-I, lane B1). As such, aminoacylation with glutamate would allow us to examine any tRNA (other than tRNA^{Glu}) that can be oxidized to form a complex with GluRS. As shown in Figure 1-I, lane B2, no complexes were observed in this case. These controls indicate that only tRNA$_{OX}^{Glu}$ is able to form covalent
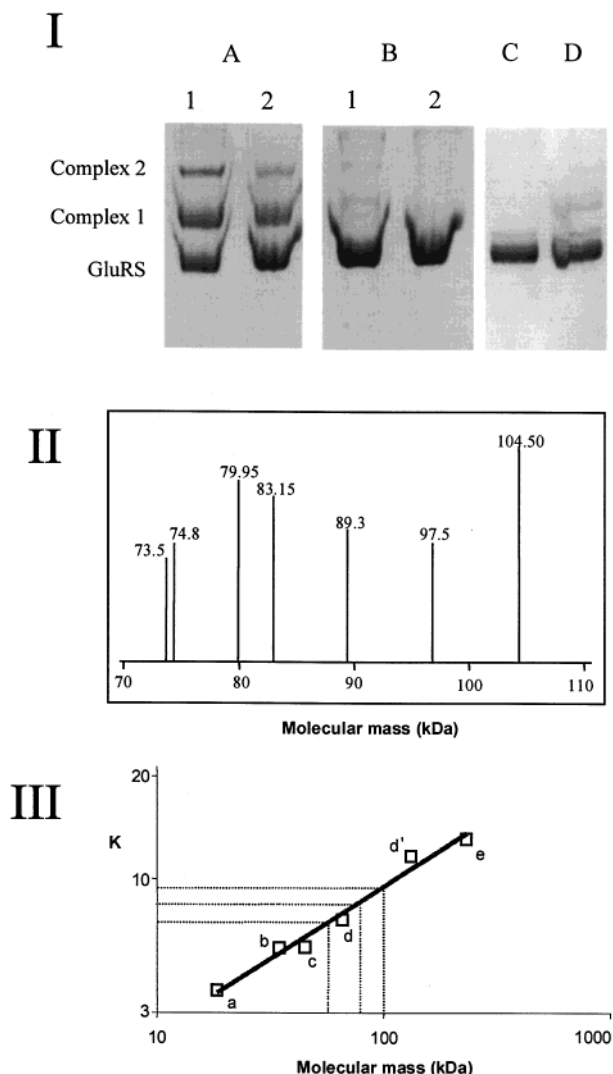
FIGURE 1: Purification and characterization of the covalent complexes formed between *E. coli* tRNA$_{OX}^{Glu}$ and GluRS. (I) By SDS−PAGE: on gel B, tRNA was aminoacylated with glutamate prior to oxidation. On lane 1 of both gels, we used pure tRNA^{Glu}; on lane 2, unfractionated tRNA enriched for tRNA$_2^{Gln}$ was used. In gel D, the complexes were formed under equilibrium conditions using NABH$_4$ instead of NaCNBH$_3$ (see Experimental Procedures), and gel C is GluRS alone. Complex 1 and complex 2 are respectively the 1:1 and the 1:2 GluRS−tRNA$_{OX}^{Glu}$ covalent complexes. Molecular masses of the tRNA$_{OX}^{Glu}$−GluRS complexes were determined by ESI mass spectrometry (II) (see Experimental Procedures) and by electrophoresis under nondenaturing conditions (III) (*15*). The complexes and five molecular mass markers were analyzed by electrophoresis on six gels containing from 4 to 12% polyacrylamide. Markers were (a) *β*-lactoglobulin (18.4 kDa), (b) pepsin (34.7 kDa), (c) egg albumin (45 kDa), (d) bovine serum albumin (66 kDa), (d′) its dimer (132 kDa), and (e) catalase (232 kDa). *K* is minus the slope of the mobility {100[log ($R_f \times$ 100)]} vs the percentage of acrylamide. *K* values were 7.31 for GluRS and 8.35 and 9.25 for the GluRS−tRNA complexes, which gives molecular masses of 54, 73, and 94 kDa.

complexes with GluRS. In a more general fashion, the formation of covalent complexes between a tRNA and its synthetase and the facile isolation of the complex suggest a powerful tool to select tRNAs (e.g., mutants) recognized by an aaRS.

Besides GluRS, the formation of two covalent complexes following the reaction of a periodate-oxidized tRNA and its cognate aaRS has also been observed for synthetases specific
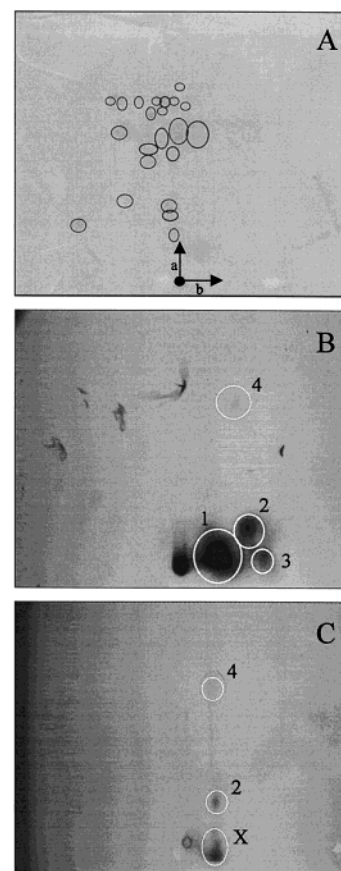

FIGURE 2: Isolation of the tryptic peptides of *E. coli* GluRS that are cross-linked to the C-C-^{32}P-A from tRNA$_{OX}^{Glu}$. The black circle on panel A is the origin. The first migration (a) was an ascending chromatography in ethanol/chloroform/28% ammonia/water (5:2:1:1). The second migration (b) was an electrophoresis in ammonium acetate (100 mM, pH 8). (A) 15 *μ*mol of peptides resulting from the digestion of pure GluRS was separated and stained with ninhydrin. (B) Autoradiogram of the digested complex 1. (C) Autoradiogram of the digested complex 2.

for arginine (*20*) and for glutamine (Madore, Gagnon, and Lapointe, unpublished results). The three enzymes, GluRS, GlnRS, and ArgRS, are known for their dependence on binding to their cognate tRNA in order to proceed with the amino acid activation step. Enzymes such as MetRS, PheRS, TyrRS, and AlaRS, which do not require tRNA to proceed with the amino acid activation step, are not known to form a 1:2 complex (*10*, *21−26*). As we show here, because the GluRS−tRNA^{Glu} 1:2 complex represents a substantial fraction of the reaction complex, its significance cannot be overlooked. The fact that the cross-linking assay was a nonequilibrium reaction may explain the appearance of the 1:2 complex. Under these conditions, as soon as a Schiff base is formed, it is stabilized by NaCNBH$_3$, thus freezing the tRNA on the enzyme and pulling the reaction toward the products. Additionally, the 1:1 complex may undergo a conformational change to allow the binding of a second tRNA to form the 1:2 complex. It is conceivable that a tRNA may get out of its binding site but still remain covalently bound to the GluRS, leaving space for a second tRNA. To see what happens under equilibrium conditions, we allowed the enzyme and the oxidized tRNA to form complexes and react in the absence of a reducing agent, and we stopped the reaction by adding 0.1 M NaBH$_4$, which stabilizes the Schiff base and reduces the oxidized tRNA. Under these conditions,

Table 1: Sequence of the *E. coli* GluRS Peptides Cross-Linked to the 3′-End of Periodate-Oxidized tRNA^{Glu}

source	spot	cross-linked peptides[a]	relative amount[b]
plate A, pure GluRS		none	N/A
plate B, complex 1	2	^{41}IEDTDLER^{48}	0.75
	3	^{110}EEQMAK^{115}	1.0
	1	^{200}GEDHINNTPR^{209}	0.41
	4	^{363}YFYEDFAEFDADAAK^{377}	<0.1
plate C, complex 2	2	^{41}IEDTDLER^{48}	0.64
	X	??	??
	4	^{82}YNAVIDQMLEEGTAYK^{97}	<0.1
	4	^{363}YFYEDFAEFDADAAK^{377}	<0.1

[a] No other peptides were detected. [b] Amounts of amino acids measured in the fourth cycle of Edman degradation, relative to those found for spot 3 where 69 pmol of PTH-methionine was found. The difference between the relative amounts of peptides measured by this method and the size of the spots on Figure 2 may come from peptides whose sequencing were difficult to determine (such as spot X) because they are too short or N-blocked.

only one complex was formed (Figure 1-I, lane D). To confirm that no 1:2 complex was there, we used a more sensitive approach; we did the same experiment using 2 μM GluRS and 4 μM ^{32}P-labeled tRNA^{Glu} and observed no 1:2 complex on the autoradiogram (data not shown). These results indicate that the 1:2 complex is very unlikely to exist in vivo. Still, the fact that this 1:2 complex can be formed indicates that the CCA-binding region is able to accommodate two CCA-ends.

Identification of the GluRS Residues Cross-Linked to the 3′-End of tRNA^{Glu}. Both complexes were purified by SDS−PAGE and digested with RNase T1, which leaves only the CC-^{32}P-A covalently linked to the enzyme. The resulting labeled GluRS was digested with trypsin, and the peptides were analyzed by two-dimensional thin-layer chromatography. The radiolabeled peptides from each complex migrated at positions free of any unlabeled peptides (Figure 2). We extracted the labeled peptides from both complexes (Figure 2B,C) and sequenced each of them by Edman degradation. No peptides were found on plate A at these positions, showing that the radioactive spots on panels B and C can only be modified CC-^{32}P-A-peptides. The large number of peptides obtained on plate A (Table 1) and the fact that the fragments just upstream or downstream of the radiolabeled ones are not seen indicate that the digestion was complete. Indeed, in the case of a partial digestion, the major peptide ^{200}GEDHI... would have been accompanied by ^{175}TDGSP... (if digestion at Arg199 was partial) and by ^{210}QINIL (if Lys215 was the cross-linking site and the digestion at Arg209 was partial) (Figure 3), but peptides with these N-terminal sequences were not found. Comparison of the cross-linked sequences with that of *E. coli* GluRS showed that two of the three major peptides, IEDTD... and GEDHI..., were cross-linked to arginine rather than to the expected lysine. Although previously characterized covalent complexes between periodate-oxidized tRNAs and aaRSs usually involved the primary amine group of lysine residues (*22−24*), cross-linking with an arginine was also reported by Hountondji et al. (*27*). In summary, analysis of cross-links identified large amounts of Arg48, Lys115, and Arg209 and trace amounts of Lys377 and Lys97; we will designate them respectively "major" and "minor" cross-linked residues.

Location of the Cross-Linked Residues in the Three-Dimensional Structure of the GluRS−tRNA^{Glu} Complex. We analyzed the cross-linked residues in both the 1:1 and 1:2 complexes. The analysis was achieved by structural modeling of *E. coli* GluRS based upon the known crystal structure of *T. thermophilus* GluRS (*5*). Because the two enzymes share 37% amino acid identity, structural modeling was relatively straightforward. The position of *E. coli* tRNA^{Glu} was modeled according to that of *E. coli* tRNA^{Gln} on *E. coli* GlnRS in the known crystal structure of the complex (*4*). Because the structure of the N-terminal half of GlnRS is similar to that of *T. thermophilus* GluRS (*5*), we superimposed the first halves of these two synthetases, using the Homology program of Insight II. Their Rossmann folds are nearly structurally identical and can be easily superimposed; the fact that this region provides the binding site for the tRNA acceptor end validates this modeling study. It showed that *E. coli* tRNA$_2^{Gln}$ fits remarkably well in the active site of the GluRS except for some minor bumps in the D-arm. These results are consistent with those obtained in the modeling of *T. thermophilus* tRNA^{Glu} (*28*), and with the presence of major identity determinants in the "augmented D helix" of *E. coli* tRNA^{Glu} (*29*). Once the model of the complex of tRNA^{Glu} with GluRS was built, we then identified the cross-linked peptides in the model.

The 1:1 GluRS−tRNA$_{OX}^{Glu}$, identified as "complex 1", revealed three major peptides and a minor one. In our model, the three major cross-linked residues on *E. coli* GluRS are Arg48, Arg209, and Lys115, which correspond to Arg47, Ile215, and Lys117 of *T. thermophilus* GluRS, respectively (Figure 3). These residues are shown as yellow in the 3D model of the *E. coli* tRNA$_2^{Gln}$−*T. thermophilus* GluRS complex (Figure 4). The minor cross-linked residue, Lys377, corresponds to Arg385 on *T. thermophilus* GluRS. Lys115 of *E. coli* GluRS is in the Cys100−Cys125 loop closed by the coordination of Cys98, Cys100, Cys125, and His127 to a zinc atom and located in the tRNA acceptor stem-binding domain (*30*). As this residue is in a small insertion in the alignment with *T. thermophilus* GluRS, we used Lys117 as the corresponding residue for our model because it is at the beginning of that insertion. Hountondji et al. (*27*) also reported cross-linking of the 3′-end ribose of shortened oxidized tRNA^{Met} with the zinc-binding region of *E. coli* MetRS (*31*). Thus, the zinc-binding regions of these two class I aminoacyl-tRNA synthetases may have similar roles in binding the CCA-ends of their cognate tRNAs.

The validity of our model for the 1:1 complex is supported by the finding that Arg47 (in the acceptor stem cleft) is proximal to the ribose of A76. This position can easily explain the facile cross-linking of Arg47 in the *E. coli* tRNA$_{OX}^{Glu}$−GluRS complex. The other two major cross-linked residues, Arg209 and Lys115 (corresponding to Ile215 and Lys117 in *T. thermophilus* GluRS), were also located in the acceptor stem cleft (Figure 4). The minor cross-linked residue, Lys377 in *E. coli* GluRS, is near the anticodon-binding domain. This location could be due to the presence of a small amount of the dimer of tRNA^{Glu} which is in equilibrium with an inactive conformer (*32*). In this dimer, the tRNA^{Glu} molecules are antiparallel (*33*); therefore, if a small amount of this dimer was present under our cross-linking conditions, the acceptor stem of one tRNA would

```
              αA          β2                            αB
Glueco    30  ARNHGGEFVL  RIEDTDLERS  TPEAIEAIMD  GMNWLSLEWD  69
Glutth    29  ARRNGGRFIV  RIEDTDRARY  VPGAEERILA  ALKWLGLSYD  68
Glneco    54  AQDYKGQCNL  RFDDTNPVKE  DIEYVESIKN  DVEWLGFHWS  93

                  β4              αD                    αE
Glueco    90  LEEGTAYKCY  CSKERLEALR  EEQMAKGEKP  RYDGRCRHSH  129
Glutth    97  LKRGWAYRAF  ETPEELEQIR  K......EKG  GYDGRARNIP  130
Glneco   114  INKGLAYVDE  LTPEQIREYR  GTLTQPGKNS  PYRDRSVEEN  153

               β8                    β9         αG          β10
Glueco   170  LIIRRTDG..  ..........  SPTYNFCVVV  DDWDMEITHV  197
Glutth   176  VVLLKSDG..  ..........  YPTYHLANVV  DDHLMGVTDV  203
Glneco   188  PVLYRIKFAE  HHQTGNKWCI  YPMYDFTHCI  SDALEGITHS  227

              β10              αH
Glueco   198  IRGEDHINNT  PRQINILKAL  217
Glutth   204  IRAEEWLVST  PIHVLLYRAF  223
Glneco   228  LCTLEFQDNR  RLYDWVLDNI  247
```

FIGURE 3: Alignment of amino acid sequences of *E. coli* GluRS (Glueco), *T. thermophilus* GluRS (Glutth), and *E. coli* GlnRS (Glneco) in the regions of the major cross-links with the 3′-end of tRNA^Glu in the 1:1 complex. The α-helices and the β-strands of *T. thermophilus* GluRS (*5*) are identified.
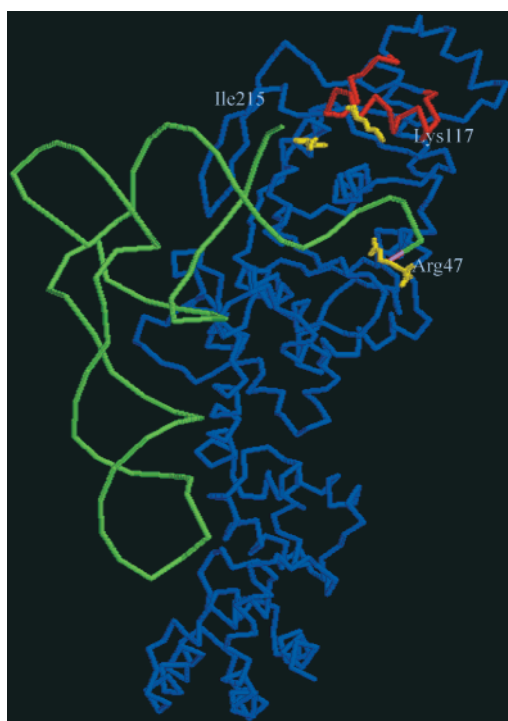

FIGURE 4: *E. coli* tRNA$_2^{Gln}$ on the active site of *T. thermophilus* GluRS used as a model for the *E. coli* tRNA^Glu−GluRS complex. In pink, the A76 nucleotide. In yellow, the three residues that were cross-linked to the 3′-end of tRNA$_{OX}^{Glu}$; the highest one is Lys117, the middle one is Ile215, and the lowest one is Arg47. The Cys98−His125 loop closed by a zinc atom is shown in red.

be near the anticodon when that of the other is at the active site.

In the 1:2 complex, two of the cross-linked residues (Arg48 and Lys377) are also present in the 1:1 complex (Table 1). A third one, Lys97, is in the acceptor stem-binding domain immediately adjacent to the Cys100−His125 loop (see above). No clear sequence was obtained by Edman degradation of the material present in the remaining major spot "X" on plate 2C (Figure 2; see also the footnotes to

Table 1). These results suggest that in the 1:2 complex, one of the tRNAs is bound to GluRS as in the 1:1 complex; however, more information will be needed to locate the second tRNA molecule.

Model(s) Consistent with the Existence of Three Major Sites in E. coli GluRS Cross-Linked with the 3′-End of tRNA$_{OX}^{Glu}$ in the 1:1 Complex.

(A) *First Model: Several Mobile Parts of the Synthetase Reach a Rigid Acceptor End of tRNA^Glu*. In this model, we placed the tRNA^Glu at the active site (as in Figure 4) and tried to find a way to bend the GluRS enough to make Lys117 and Ile215 (on *T. thermophilus* GluRS) reach the oxidized ribose. It may be possible to move Ile215 enough to reach the ribose but only at the expense of a substantial rearrangement of the active site. On the other hand, it is not possible to make Lys117 (Figure 4, the uppermost yellow residue above the acceptor stem) reach the 3′-terminal ribose without destroying the active site. Therefore, we did not consider this model further.

(B) *Second Model: The 3′-End of tRNA^Glu Is Mobile in Solution, which Gives Several Docking Sites for the GCCA End.* The solution structure of several acceptor stems with a purine as a discriminator base shows that these nucleotides are stacked on the stem in a A-helix conformation; this is true for yeast tRNA^Phe as revealed by its 3D structure determined by X-ray diffraction (*34, 35*), and the acceptor helix of several tRNAs as determined by NMR. These acceptor helices include the *E. coli* tRNA^Ala microhelix (*36*), the *E. coli* tRNA^fMet microhelix variant containing a G1·C72 base pair in place of the C1·A72 mismatch in *E. coli* tRNA^fMet (*37*), and the human tRNA^Leu microhelix (*38*). Furthermore, studies of the human tRNA^Leu microhelix indicate the presence of only one conformer, with its 3′-end single-stranded segment in an A-helix conformation and stacked on the acceptor stem. The conformation of the 3′-end may also be assessed by the T4 RNA ligase catalyzed circularization of tRNA (*16*). Previous studies indicate that a U73-containing *E. coli* tRNA^Cys is circularized much faster than the A73 variant of *E. coli* tRNA^Cys. The faster rate of
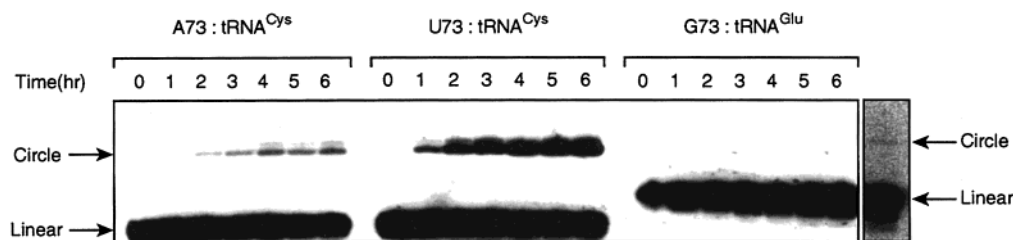
FIGURE 5: Circularization of tRNA by T4 RNA ligase as an indicator for the flexibility of the CCA end. The time course of the circularization is shown for an A73-containing tRNA (the A73 variant of *E. coli* tRNA^{Cys}, A73:tRNA^{Cys}), a U73-containing tRNA (the wild-type *E. coli* tRNA^{Cys}, U73:tRNA^{Cys}), and the G73-containing *E. coli* tRNA^{Glu} (G73:tRNA^{Glu}). The migration positions of the circular form and of the linear form are indicated by arrows. Analysis of the kinetics of circularization indicates that the A73-containing tRNA reached a plateau of 9.3%, the U73-containing tRNA reached a plateau of 26.8%, and the G73-containing *E. coli* tRNA^{Glu} reached a plateau of 0.7%. Because the amount of the circular form for tRNA^{Glu} is extremely small, it is shown (at the right) in a separate contrast relative to the rest of the gel.

circularization of the U73-containing tRNA is consistent with the ability of the CCA end to foldback toward the 5′-end of the acceptor stem. The slower rate of circularization of the A73 variant is consistent with the helical stacking of the CCA end (*16*). The fact that the G73 variant has the same rate of circularization as the A73 variant (*16*) suggests that the conformation of the GCCA end is likely to be stacked. We used this approach to determine the conformation of the GCCA end of *E. coli* tRNA^{Glu} (Figure 5). After 6 h of incubation in the presence of T4 RNA ligase, less than 1% of *E. coli* tRNA^{Glu} is circularized as compared to 26.8% for *E. coli* U73·tRNA^{Cys} and 9.3% for *E. coli* A73·tRNA^{Cys}. The circularization rate of this tRNA is also much slower than those of *E. coli* tRNA^{Ala} and yeast tRNA^{Asp}, which are known to possess an extended 3′-end (*1, 16, 39*). This indicates that the *E. coli* tRNA^{Glu} GCCA end is in an extended conformation, probably helical and stacked on the acceptor stem. The proposed helical stacking of the GCCA end of *E. coli* tRNA^{Glu} is supported by biochemical studies. In the tRNA^{Glu} variant C72A, the 3′-end is destabilized by the loss of the first base pair of its acceptor stem. The increased flexibility should, in the context of this second model, increase the frequency of the collisions between the 3′-terminal ribose of tRNA and the active site, and hence increase the k_{cat} value of the aminoacylation reaction. However, results indicate that this mutation decreases k_{cat} by 60-fold (*29*). These results indicate that the three major cross-links observed do not result from the reaction of three different conformers of tRNA^{Glu} in solution with GluRS.

(C) Third Model: The 3′-End of tRNA^{Glu} Unfolds on GluRS. It is known that tRNA molecules can undergo several conformational changes when they dock their aaRS, particularly in their acceptor stems. For instance, yeast tRNA^{Asp} conformation changes when it binds to AspRS (*40*). Also, the CCA end of *E. coli* tRNA^{Gln} in the complex with GlnRS is bended rather than extended as observed in the ligand-free yeast tRNA^{Phe} (*3, 41*). This suggests the possibility of conformational changes in the end of the acceptor stem and in the single-stranded 3′-end segment. Given this possibility and the specificity of the cross-linked complexes (see Figure 1-I), we suggest a model in which the acceptor end of tRNA^{Glu} unfolds on GluRS from its extended helical conformation to a foldback conformation as observed in the complex of tRNA^{Gln}−GlnRS. In this unfolding process, the CCA end would sweep across the three major sites identified by cross-links (Figure 6), while keeping the overall interactions between tRNA^{Glu} and GluRS untouched as they define

the specificity for tRNA^{Glu} (*29*).

We modeled the initial contact of tRNA^{Glu} on GluRS based on the known structure of free tRNA^{Phe} from yeast (*3, 41*). We modeled the final contact by using tRNA^{Gln} in the tRNA^{Gln}−GlnRS complex. In the initial contact, the extended and helical GCCA end is such that the reactive *cis*-diol of its terminal ribose is near Lys117 (Figure 6A,A′). As *E. coli* GluRS has a small insertion at this position, compared to *T. thermophilus* GluRS, our model may be slightly imprecise in this area. However, this imprecision should not invalidate the model because there is plenty of room around the CCA end in the initial contact. It is conceivable that tRNA^{Glu} can adapt to the small perturbation brought by this insertion. In the final contact, the ribose of A76 is placed near Arg47. This position is achieved by folding the CCA end in a way analogous to that of tRNA^{Gln} in the complex with GlnRS (*4*) (Figure 6C,C′). In this "final" conformation, A76 is positioned in the active site. The remaining major cross-linked site (Ile215 for *T. thermophilus* GluRS, Arg209 for *E. coli* GluRS) corresponds in this model to an intermediate between the initial and the final conformations. The transition between this stage and the final one can be made by a few rotations around the phosphates of nucleotides 74 and 76. Several different conformational changes of the GCCA segment would allow the ribose of A76 to sweep the interior of the pocket and to reach Ile215 (Figure 6B,B′). From there, only a small displacement is needed to reach the final state (Figure 6C,C′). All these movements of the 3′-terminal GCCA segment of tRNA^{Glu} in the acceptor cleft of the synthetase can be done without significant disruption of the tRNA−synthetase complex. Our data do not exclude the possibility of conformational changes of GluRS during this unfolding.

In this third model, we detected one intermediate between the initial and final conformations. However, there may be other intermediates that are not trapped by cross-links. Previous studies (*42*) indicate that the unfolding of the CCA end would proceed faster than cross-link formation. The latter must go through the formation of a Schiff base between the oxidized tRNA and a lysine or arginine on the enzyme. The chemistry of formation of a Schiff base involves the elimination of a water molecule and thus is intrinsically slower (*43*) than the unfolding of the CCA end which does not involve alteration of chemical bonds.

In summary, the cross-linking of the 3′-end of tRNA^{Glu} to GluRS reveals a model that is reminiscent of the model of tRNA^{Gln} complexed with GlnRS. This is perhaps not surpris-
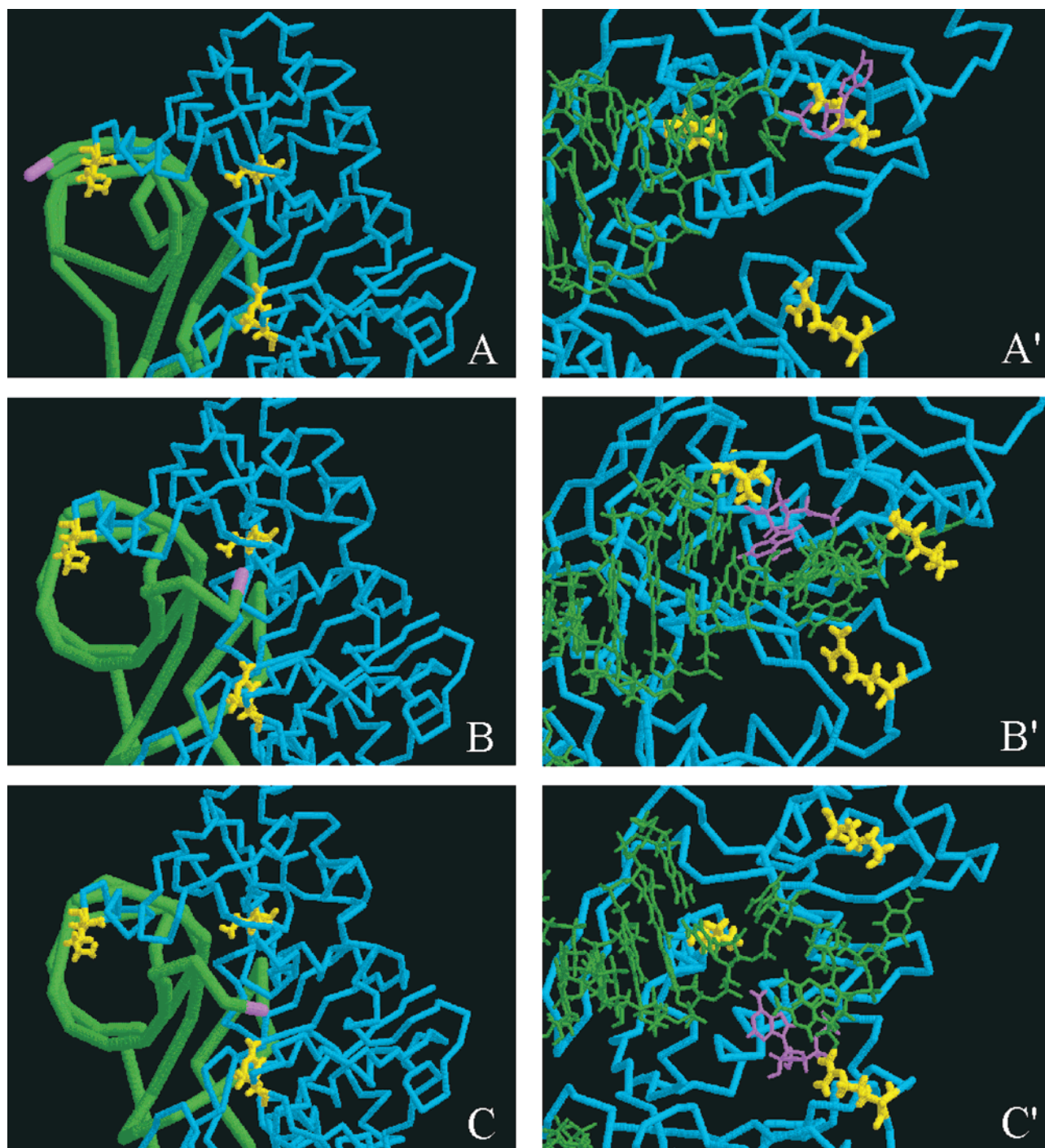
FIGURE 6: Steps in the unfolding of tRNA^Glu on GluRS. In panels A, B, and C, we see the end of tRNA^Glu unrolling from its A-helix stacked conformation (A) to that seen in the tRNA_2^Gln−GlnRS complex (C); an intermediate conformation revealed by the cross-linking to Arg209 is shown in panel B. Panels A′, B′, and C′ show more details of the contacts between the A76 nucleotide and the cross-linked peptides. tRNA is colored in green, GluRS in blue, A76 in pink, and cross-linked residues in yellow.

ing given the structural similarity and the strong evolutionary relationships between GluRS and GlnRS (reviewed in *44*). In both complexes, the 3′-end of the tRNA is bended and placed in the active site of the enzyme. However, our study provides insights into the formation of the final complex that are additional to those provided by the crystal structure of the *E. coli* GlnRS−tRNA^Gln complex. Specifically, we suggest that the tRNA in the initial contact with the synthetase maintains an extended helical 3′-end and that this extended conformation unfolds on the enzyme to reach the final conformation. To the best of our knowledge, although

the crystal structure of GlnRS complexed with tRNA^Gln showed a foldback structure of the tRNA 3′-end, there are no biochemical data that directly tested the pathway of the foldback. Thus, as our work provides evidence for the unfolding of the 3′-end of tRNA^Glu on GluRS, it adds new insights into the dynamics of the tRNA−synthetase complexes.

Kinetic analysis of the proposed unfolding will be useful to test further our model, but the rate of this unfolding is probably too fast to follow it with a cross-linking reaction. On the other hand, our results open the door to the design

of GluRS (and eventually of GlnRS) variants that are altered in residues along the proposed pathway. The substitutions of these residues are expected to affect the kinetics of aminoacylation; thus, kinetic analyses of such variants and cross-linking of these variants to tRNA^{Glu} should allow us to strengthen and refine our model.

ACKNOWLEDGMENT

REFERENCES

1. Ruff, M., Krishnaswamy, S., Boeglin, M., Poterszman, A., Mitschler, A., Podjarny, A., Rees, B., Thierry, J. C., and Moras, D. (1991) *Science 252*, 1682−1689.
2. Westhof, E., Dumas, P., and Moras, D. (1985) *J. Mol. Biol. 184*, 119−145.
3. Kim, S. H., Suddath, F. L., Quigley, G. J., McPherson, A., Sussman, J. L., Wang, A. H. J., Seeman, N. C., and Rich, A. (1974) *Science 185*, 435−440.
4. Rould, M., Perona, J., Söll, D., and Steitz, T. (1989) *Science 246*, 1135−1142.
5. Nureki, O., Vassylyev, D. G., Katayanagi, K., Shimizu, T., Sekine, S., Kigawa, T., Miyazawa, T., Yokoyama, S., and Morikawa, K. (1995) *Science 267*, 1958−1965.
6. Lin, S. X., Brisson, A., Liu, J., Roy, P., and Lapointe, J. (1992) *Protein Expression Purif. 3*, 71−74.
7. Bishoff, R., and McLaughlin, L. W. (1985) *Anal. Biochem. 151*, 526−533.
8. Perona, J. P., Swanson, R., Steitz, T. A., and Söll, D. (1988) *J. Mol. Biol. 202*, 121−126.
9. Cudny, H., and Deutscher, M. P. (1986) *J. Biol. Chem. 261*, 6450−6453.
10. Fayat, G., Hountondji, C., and Blanquet, S. (1979) *Eur. J. Biochem. 96*, 87−92.
11. Kern, D., and Lapointe, J. (1980) *J. Biol. Chem. 255*, 1956−1961.
12. Murray, M. C., Bhavanandan, V. P., Davidson, E. A., and Reinhold, V. (1989) *Carbohydr. Res. 186*, 255−265.
13. Puri, K. D., and Springer, T. A. (1996) *J. Biol. Chem. 271*, 5404−5413.
14. Laemmli, U. K. (1970) *Nature 227*, 680−685.
15. Mueller, J. E., Smith, D., Bryk, M., and Belfort, M. (1995) *EMBO J. 22*, 5724−5735.
16. Hou, Y. M., Lipman, R. S., and Zarutskie, J. A. (1998) *RNA 7*, 733−738.
17. Silberklang, M., Gillum, A. M., and RajBhandary, U. L. (1979) *Methods Enzymol. 59*, 58−109.
18. Devereux, J., Haeberli, P., and Smithies, O. (1984) *Nucleic Acids Res. 12*, 387−395.
19. Fitzgerald, M. C., and Smith, L. M. (1995) *Annu. Rev. Biophys. Biomol. Struct. 24*, 117−140.
20. Cheng, X., Lin, S., Shi, J., and Wang, Y. (1991) *Sci. China 34*, 293−305.
21. Renaud, M., Fasiolo, F., Baltzinger, M., Boulanger, Y., and Remy, P. (1982) *Eur. J. Biochem. 123*, 267−274.
22. Hountondji, C., Blanquet, S., and Lederer, F. (1985) *Biochemistry 24*, 1175−1180.
23. Hountondji, C., Lederer, F., Dessen, P., and Blanquet, S. (1986) *Biochemistry 25*, 16−21.
24. Hountondji, C., Schmitter, J. M., Beauvallet, C., and Blanquet, S. (1987) *Biochemistry 26*, 5433−5439.
25. Hill, K., and Schimmel, P. (1989) *Biochemistry 28*, 2577−2586.
26. Sanni, A., Hountondji, C., Blanquet, S., Ebel, J. P., Boulanger, Y., and Fasiolo, F. (1991) *Biochemistry 30*, 2448−2453.
27. Hountondji, C., Schmitter, J. M., Beauvallet, C., and Blanquet, S. (1990) *Biochemistry 29*, 8190−8198.
28. Tateno, M., Nureki, O., Sekine, S., Kaneda, K., Go, M., and Yokoyama, S. (1995) *FEBS Lett. 377*, 77−81.
29. Sekine, S., Nureki, O., Sakamoto, K., Niimi, T., Tateno, M., Go, M., Kohno, T., Brisson, A., Lapointe, J., and Yokoyama, S. (1996) *J. Mol. Biol. 256*, 685−700.
30. Liu, J., Gagnon, Y., Gauthier, J., Furenlid, L., L'Heureux, P. J., Auger, M., Nureki, O., Yokoyama, S., and Lapointe, J. (1995) *J. Biol. Chem. 270*, 15162−15169.
31. Fourmy, D., Dardel, F., and Blanquet, S. (1993) *J. Mol. Biol. 231*, 1078−1089.
32. Eisinger, J., and Gross, N. (1975) *Biochemistry 14*, 4031−4041.
33. Madore, E., Florentz, C., Giege, R., and Lapointe, J. (1999) *Nucleic Acids Res. 27*, 3583−3588.
34. Ladner, J. E., Jack, A., Robertus, J. D., Brown, R. S., Rhodes, D., Clark, B. F., and Klug, A. (1975) *Proc. Natl. Acad. Sci. U.S.A. 72*, 4414−4418.
35. Suddath. F. L., Quigley, G. J., McPherson, A., Sneden, D., Kim, J. J., Kim, S. H., and Rich, A. (1974) *Nature 248*, 20−24.
36. Ramos, A., and Varani, G. (1997) *Nucleic Acids Res. 25*, 2083−2090.
37. Puglisi, E. V., Puglisi, J. D., Williamson, J. R., and RajBhandary, U. L. (1994) *Proc. Natl. Acad. Sci. U.S.A. 91*, 11467−11471.
38. Metzger, A. U., Heckl, M., Willbold, D., Breitschopf, K., RajBhandary, U. L., Rosch, P., and Gross, H. J. (1997) *Nucleic Acids Res. 25*, 4551−4556.
39. Limmer, S., Hofmann, H. P., Ott, G., and Sprinzl, M. (1993) *Proc. Natl. Acad. Sci. U.S.A. 90*, 6199−6202.
40. Rees, B., Cavarelli, J., and Moras, D. (1996) *Biochimie 78*, 624−631.
41. Robertus, J. D., Ladner, J. E., Finch, J. T., Rhodes, D., Brown, R. S., Clark, B. F. C., and Klug, A. (1974) *Nature 250*, 546−551.
42. Cantor, C. R., and Schimmel, P. R. (1980) *Biophysical Chemistry*, pp 1211−1214, W. H. Freeman and Co., New York.
43. Streitwieser, A., and Heathcock, C. (1985) *Introduction to Organic Chemistry*, 3rd ed., pp 384−385, MacMillan Publishing Co., New York.
44. Freist, W., Gauss, D. H., Söll, D., and Lapointe, D. (1997) *Biol. Chem. 378*, 1313−1329.